Journal of Medicinal Chemistry

Article

pubs.acs.org/jmc

Synthesis and Evaluation of 1,5-Disubstituted Tetrazoles as Rigid Analogues of Combretastatin A-4 with Potent Antiproliferative and Antitumor Activity

Romeo Romagnoli,*[,†] Pier Giovanni Baraldi,*[,†] Maria Kimatrai Salvador,[†] Delia Preti,[†] Mojgan Aghazadeh Tabrizi,[†] Andrea Brancale,[‡] Xian-Hua Fu,[§] Jun Li,[§] Su-Zhan Zhang,[§] Ernest Hamel,[⊥] Roberta Bortolozzi,[‡] Giuseppe Basso,[∥] and Giampietro Viola*[,∥]

[†]Dipartimento di Scienze Farmaceutiche, Università di Ferrara, 44100 Ferrara, Italy

[‡]The Welsh School of Pharmacy, Cardiff University, King Edward VII Avenue, Cardiff, CF10 3NB, U.K.

[§]Cancer Institute, Key Laboratory of Cancer Prevention and Intervention, China National Ministry of Education, The Second Affiliated Hospital, School of Medicine, Zhejiang University, Hangzhou, Zhejiang Province 310009, People's Republic of China

[∥]Laboratorio di Oncoematologia, Dipartimento di Pediatria, Università di Padova, 35131 Padova, Italy

[⊥]Screening Technologies Branch, Developmental Therapeutics Program, Division of Cancer Treatment and Diagnosis, National Cancer Institute at Frederick, National Institutes of Health, Frederick, Maryland 21702, United States

ABSTRACT: Tubulin, the major structural component of microtubules, is a target for the development of anticancer agents. Two series of 1,5-diaryl substituted 1,2,3,4-tetrazoles were concisely synthesized, using a palladium-catalyzed cross-coupling reaction, and identified as potent antiproliferative agents and novel tubulin polymerization inhibitors that act at the colchicine site. SAR analysis indicated that compounds with a 4-ethoxyphenyl group at the N-1 or C-5 position of the 1,2,3,4-tetrazole ring exhibited maximal activity. Several of these compounds also had potent activity in inhibiting the growth of multidrug resistant cells overexpressing P-glycoprotein. Active compounds induced apoptosis through the mitochondrial pathway with activation of caspase-9 and caspase-3. Furthermore, compound **4l** significantly reduced in vivo the growth of the HT-29 xenograft in a nude mouse model, suggesting that **4l** is a promising new antimitotic agent with clinical potential.

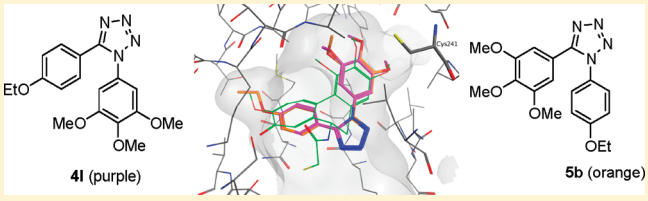

INTRODUCTION

Microtubules are a key component of the cytoskeleton, and they are involved in a wide range of cellular functions, including regulation of motility, cell division, organelle transport, maintenance of cell morphology, and signal transduction.[1] The essential role of microtubules in mitotic spindle formation and proper chromosomal separation makes them one of the most attractive targets for the design and development of many small natural and synthetic antitumor drugs.[2] Many of them exert their effects by inhibiting the noncovalent polymerization of tubulin into microtubules. Therefore, there has been great interest in identifying and developing novel antimicrotubule molecules. Among the naturally occurring compounds, combretastatin A-4 (**1**, Chart 1) is one of the best characterized antimitotic agents. Combretastatin A-4, isolated from the bark of the South African tree *Combretum caffrum*,[3] is a highly effective natural tubulin-binding molecule affecting microtubule dynamics by binding to the colchicine site.[4] **1** shows potent cytotoxicity against a wide variety of human cancer cell lines, including those that are multidrug resistant, based on overexpressing P-glycoprotein (P-gp).[5] A water-soluble disodium phosphate derivative of **1** (named combretastatin A-4 phosphate) has shown promising results in human cancer clinical trials,[6] thus stimulating significant interest in a variety of combretastatin A-4 analogues.[7]

Previous SAR studies with analogues of **1** showed that both the 3′,4′,5′-trimethoxy substitution pattern on the A-ring and the *cis*-olefin configuration at the bridge were essential for optimal activity, while B-ring structural modifications were tolerated by the target.[7] Despite the remarkable anticancer activity of **1**, the cis-configured double bond is prone to isomerize to the chemically more stable trans form during storage and metabolism, resulting in a dramatic loss in antitumor activity. Thus, to retain the appropriate configuration of the two adjacent aryl groups required for bioactivity, heterocombretastatin derivatives with general structure **2** were obtained by replacing the stilbene core of **1** with 1,2-diaryl substituted five-member aromatic heterocyclic rings, such as thiophene,[8] furan,[8] pyrazole,[9] imidazole,[9,10] thiazole,[9a] isoxazole,[11] 1,2,3-thiadiazole,[12] and isomeric triazoles.[9,13]

Recently, we described a series of 1,5-diaryl-1,2,4-triazoles, with general structure **3**, as potent inhibitors of cell growth with antimitotic activity.[13c] Among the synthesized compounds,

Received: October 18, 2011
Published: December 2, 2011

   dx.doi.org/10.1021/jm2013979 | *J. Med. Chem.* 2012, 55, 475–488

Chart 1. Inhibitors and Potential Inhibitors of Tubulin Polymerization

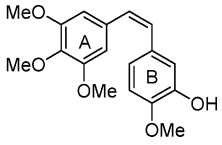

Combretastatin A-4, **1**

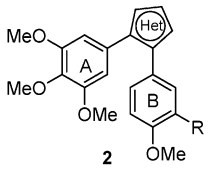

2

R=OH or NH_2
Het=thiophene, furan, imidazole; pyrazole; thiazole;oxazole; isoxazole; 1,2,3-thiadiazole; triazole, tetrazole.

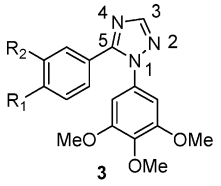

3

3a, R_1=OCH_2CH_3, R_2=H
3b, R_1=OCH_2CH_3, R_2=Cl

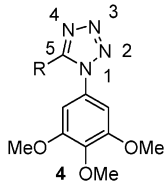

4

4a, R=C_6H_5
4b, R=2-thienyl
4c, R=p-CH_3OC-C_6H_4
4d, R=p-CH_3-C_6H_4
4e, R=p-CH_3CH_2-C_6H_4
4f, R=p-CH_3O-C_6H_4
4g, R=m,p-$(CH_3O)_2$-C_6H_3
4h, R=m,m',p-$(CH_3O)_3$-C_6H_2
4i, R=p-CH_3O, m-F-C_6H_4
4j, R=p-CH_3O, m-Cl-C_6H_4
4k, R=p-CH_3O, m-CH_3-C_6H_4
4l, R=p-CH_3CH_2O-C_6H_4
4m, R=p-CH_3CH_2O, m-Cl-C_6H_4
4n, R=p-$CH_3(CH_2)_2O$-C_6H_4
4o, R=p-$CH_3(CH_2)_3O$-C_6H_4
4p, R=p-$CH_3(CH_2)_4O$-C_6H_4

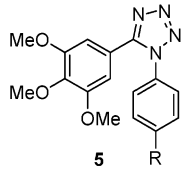

5

5a, R=OCH_3
5b, R=OCH_2CH_3

derivatives **3a** and **3b** are the most active as inhibitors of the growth of human tumor cells, with IC_{50} values of 5−100 and 3−20 nM for **3a** and **3b**, respectively. In addition, these compounds were comparable to **1** in inhibiting tubulin polymerization.

These results led us to start a pharmacophore exploration and optimization effort around the 1,2,4-triazole nucleus, replacing the CH at its C-3 position with a fourth nitrogen, to afford the bioisosteric 1,2,3,4-tetrazole derivatives with general structure **4**.[14] A noteworthy point was that the preparation of most derivatives in this series was carried out via an efficient and flexible one-step procedure, starting from a common *N*-1-(3′,4′,5′-trimethoxyphenyl)tetrazole intermediate.

For compounds **4a**−**p**, modifications were focused on varying the aryl moiety at the C-5 position of the tetrazole skeleton, corresponding to the B-ring of combretastatin A-4, by adding electron-withdrawing ($COCH_3$) or electron-releasing (alkyl and alkoxy) groups (EWG and ERG, respectively). In addition, the B-ring was replaced with a thien-2-yl moiety. Since the methoxy and ethoxy groups proved to be favorable for bioactivity, we maintained one of these substituents at the para-position and introduced an additional substituent (F, Cl, Me, or MeO) at the meta-position of the phenyl ring.

In order to understand the positional effect of the 3′,4′,5′-trimethoxyphenyl moiety on the tetrazole ring, by interchanging the 4′-alkoxyaryl and 3′,4′,5′-trimethoxyphenyl moieties at the C-5 and N-1 positions of compounds **4f** and **4l**, we synthesized the corresponding regioisomeric analogues **5a** and **5b**, respectively. Compounds **4a**−**p**, **5a**, and **5b** were characterized by the presence of a 3′,4′,5′-trimethoxyphenyl moiety, identical with the A-ring of **1**, which was considered essential for maximal tubulin binding activity.[15]

We examined the efficacy of the newly synthesized compounds on a panel of human cancer cell lines, including multidrug resistant lines overexpressing the 170 kDa P-gp drug efflux pump, and we obtained initial in vivo data on a murine xenograft nude mouse model that indicated high activity in tumor growth suppression. In addition, the mechanism of action of the most active compounds was investigated in detail.

CHEMISTRY

1,5-Aryltetrazoles **4a**−**p** and **5a**,**b** were prepared following the procedure reported in Scheme 1. The common intermediates 1-aryl substituted tetrazoles **7a**−**c**[16] were efficiently generated in a one-step procedure by the condensation of the appropriate aniline **6a**−**c** with triethyl orthoformate and sodium azide in refluxing acetic acid.[17] The subsequent regioselective bromination of **7a**−**c** with *N*-bromosuccinimide and a catalytic amount of benzoyl peroxide in refluxing CCl_4, furnished 5-bromotetrazoles **8a**−**c** with variable yields (70%, 50%, and 24% for **8a**, **8b**, and **8c**, respectively). Starting from these latter compounds, derivatives **4d**, **4i**, **4j**, **4k**, **4m**, **5a**, and **5b** were synthesized by Suzuki cross-coupling reaction with the appropriate arylboronic acid under heterogeneous conditions [$Pd(PPh_3)_4$, aqueous Na_2CO_3] in toluene at reflux.[18]

The low yield for the preparation of 5-bromotetrazole **8c** encouraged us to follow a concise and versatile synthetic approach for the synthesis of 5-aryl-1-(3′,4′,5′-trimethoxyphenyl)tetrazoles **4a**−**c**, **4e**−**h**, **4l**, and **4n**−**p** by the direct arylation of **7c** with the appropriate aryl iodide in the presence of $Pd(OAc)_2$, CuI, and $CsCO_3$, with tri-(2-furyl)-phosphine (TFP) as phosphine ligand in dry acetonitrile.[19]

dx.doi.org/10.1021/jm2013979 | *J. Med. Chem.* 2012, 55, 475−488

Scheme 1[a]

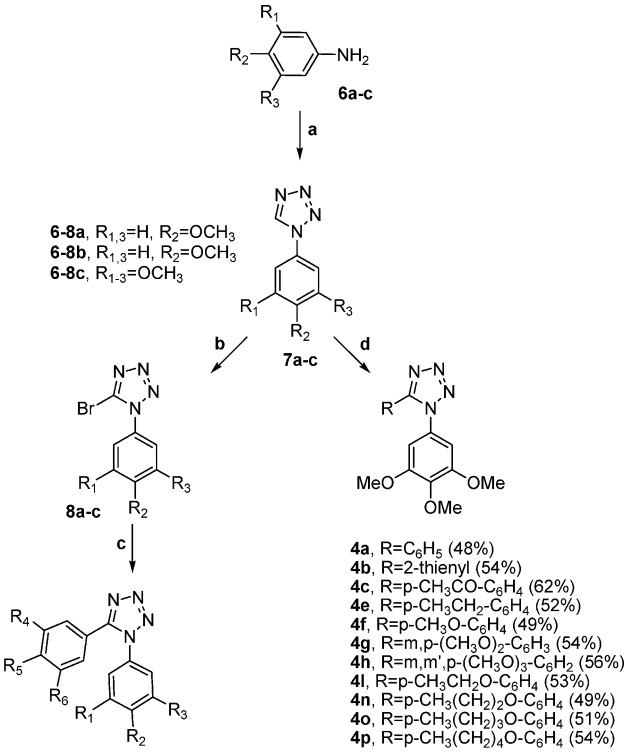

4d, $R_{1\text{-}3}=OCH_3$, $R_{4,6}=H$, $R_5=CH_3$ (56%)
4i, $R_{1\text{-}3}=OCH_3$, $R_4=F$, $R_5=OCH_3$, $R_6=H$ (49%)
4j, $R_{1\text{-}3,5}=OCH_3$, $R_4=Cl$, $R_6=H$ (52%)
4k, $R_{1\text{-}3,5}=OCH_3$, $R_4=CH_3$, $R_6=H$ (51%)
4m, $R_{1\text{-}3}=OCH_3$, $R_4=Cl$, $R_5=OCH_2CH_3$, $R_6=H$ (52%)
5a, $R_{1,3}=H$, $R_{2,4\text{-}6}=OCH_3$ (64%)
5b, $R_{1,3}=H$, $R_2=OCH_2CH_3$, $R_{4\text{-}6}=OCH_3$ (54%)

[a]Reagents: (a) NaN_3, $HC(OEt)_3$, CH_3CO_2H, reflux; (b) *N*-bromosuccinimide, benzoyl peroxide (cat.), CCl_4, reflux; (c) ArB$(OH)_2$, $Pd(PPh_3)_4$, Na_2CO_3, PhMe−H_2O−EtOH, 120 °C; (d) ArI, $Pd(OAc)_2$, CuI, TFP, $CsCO_3$, CH_3CN, 45 °C.

RESULTS AND DISCUSSION

In Vitro Antiproliferative Activities. The 1-(3′,4′,5′-trimethoxyphenyl)-5-aryltetrazoles **4a**−**p** and the corresponding regioisomeric analogues **5a** and **5b** were evaluated for their inhibition of the growth of six different human cancer cell lines in comparison with the 1,2,4-triazole derivative **3a** and the reference compound **1**. As reported in Table 1, the antiproliferative activities of the tested compounds were less pronounced against A549 cells than the other cell lines. Compound **4l**, bearing a 4′-ethoxyphenyl at the C-5 position of tetrazole ring, and its isomeric derivative **5b** exhibited the greatest antiproliferative activity among the tested compounds, with IC_{50} values of 1.3−8.1 and 0.3−7.4 nM, respectively. These values were similar to those obtained with **1** against HL-60, while **4l** and **5b** were from 2- to 1000-fold more active than **1** against the other five cell lines. While there was little difference in activity between **4l** and **5b** against each cancer cell line, this similarity did not occur with the other isomeric pair, the 4′-methoxyphenyl derivatives **4f** and **5a**. Compound **5a** was from 4- to 50-fold less active than **4f** in five of the six cancer cell lines, the exception being the MCF-7 cells, in which **5a** was somewhat more active.

Notably, by comparison of **3a** and **4l**, which shared common 3′,4′,5′-trimethoxyphenyl and 4′-ethoxyphenyl moieties at their N-1 and C-5 positions, the 1,2,3,4-tetrazole **4l** was from 8- to 31-fold more active than its 1,2,3-triazole congener **3a**, and the regioisomeric derivative **5b** was from 15- to 50-fold more active than **3a**.

The unsubstituted C-5 phenyl derivative **4a** was weakly active (IC_{50} > 0.9 μM) against all the cell lines screened, with the exception of the Jurkat cells, with which its IC_{50} was 3.8 nM. This activity against the Jurkat cells was completely lost when the phenyl moiety was replaced with the bioisosteric 2-thienyl ring (compound **4b**).

Further structural optimization was conducted with variation in the ERG or EWG on the phenyl group at the 5-position of tetrazole ring. With the exception of the Jurkat, the A549, and the MCF-7 cells, the introduction of a weak electron-withdrawing acetyl group (**4c**) produced a slight increase of activity with respect to **4a.** Comparing the two *p*-alkylphenyl derivatives **4d** and **4e**, replacing the methyl (**4d**) with an ethyl (**4e**) moiety resulted in enhanced antiproliferative activities in five of the cell lines. Both **4d** and **4e** were substantially more potent in all cells, except the Jurkat cells, than the unsubstituted **4a**. Replacement of the *p*-methyl group of **4d** with a *p*-methoxy moiety (**4f**) resulted in a 10- to 150-fold increase in antiproliferative activity. Similarly, changing the *p*-ethyl moiety of **4e** to a *p*-ethoxy group in **4l** resulted in enhanced antiproliferative activity against all six cell lines. In addition, **4l** was substantially more active than **4f** in half the cell lines (A549, Jurkat, and MCF-7 cells) and somewhat more active in the others. In combination with data where still longer *p*-alkoxy groups were examined (see below) and the data for **4e** (*p*-ethyl moiety), we conclude that the optimum length for the para-substituent appears to be three non-hydrogen atoms.

Relative to the activity of **4f**, the insertion of an additional EWG or ERG on the 3′-position of the 4′-methoxyphenyl ring had varying effects on antiproliferative activity, suggesting that steric rather than electronic factors account for the differing potencies of these compounds. A second, and especially a third, strong electron-releasing methoxy group (**4g** and **4h**, the methoxy groups present at the meta position(s)) caused substantial loss in antiproliferative activity relative to **4f**. In most of the cell lines, **4k** with the weak electron-releasing *m*-methyl group was more potent than compounds **4i** and **4j**, with the electron-withdrawing fluorine and chlorine atoms, respectively. By comparison of **4j** with **4f**, the addition of a *m*-chlorine atom in **4j** to the *p*-methoxy group in both compounds led to little change in activity in four cell lines, while **4f** was the more active in the Jurkat and the HT-29 cells. The effect of a *m*-EWG (a chlorine atom) in compound **4m** was also examined in combination with the *p*-ethoxy group of **4l**. As with the **4f** and **4j** pair, nearly identical activities were observed in most cell lines, the exception being the A549 cells, in which **4l** was the more active.

Lengthening the *p*-alkyl moiety from ethoxy (**4l**) to propoxy (**4n**) caused a significant reduction in antiproliferative activity in all cell lines. A further increase in size of this moiety (**4o** and **4p**) resulted in inactive compounds.

Inhibition of Tubulin Polymerization and Colchicine Binding. To investigate whether the antiproliferative effects of compounds **4e**−**f**, **4i**−**n**, and **5a**,**b** were derived from interactions with tubulin, these agents were evaluated for their inhibition of tubulin polymerization and for effects on the binding of [^{3}H]colchicine to tubulin (Table 2).[20] For comparison, **1** and **3a** were examined in contemporaneous experiments. In the assembly assay, compound **4l** was found to be the most active (IC_{50} = 1.1 μM), with activity being in the

dx.doi.org/10.1021/jm2013979 | J. Med. Chem. 2012, 55, 475−488

Table 1. In Vitro Cell Growth Inhibitory Effects of Compounds 1, 3a, 4a−p, and 5a,b

	IC_{50} [a] (nM)					
compd	HeLa	A549	HL-60	Jurkat	MCF-7	HT-29
4a	4097 ± 333	>10000	903 ± 123	3.8 ± 0.7	>10000	>10000
4b	>10000	>10000	>10000	>10000	>10000	>10000
4c	648 ± 211	>10000	596 ± 121	325 ± 28	>10000	6033 ± 1527
4d	255 ± 32.3	3420 ± 127	329 ± 41	222 ± 17	1785 ± 653	673 ± 43
4e	29.0 ± 5.6	3383 ± 659	53.1 ± 10	55.1 ± 4.4	12.6 ± 6.7	182 ± 60
4f	2.6 ± 0.0	222 ± 59	2.9 ± 0.6	2.6 ± 0.1	38.5 ± 5.8	4.6 ± 0.6
4g	259 ± 36.0	3574 ± 280	488 ± 71	345 ± 28	2716 ± 625	355 ± 55
4h	>10000	>10000	>10000	>10000	>10000	>10000
4i	2.8 ± 0.7	332 ± 17	7.3 ± 2.2	1.3 ± 0.1	29.7 ± 5.9	2.7 ± 0.7
4j	2.3 ± 0.5	402 ± 84	3.6 ± 0.6	10.0 ± 0.9	25.2 ± 3.4	35.9 ± 4.4
4k	2.1 ± 0.7	37.7 ± 5.0	2.0 ± 0.7	4.1 ± 0.2	15.4 ± 6.5	5.6 ± 1.5
4l	1.9 ± 0.7	8.1 ± 3.2	1.3 ± 0.3	0.16 ± 0.06	2.3 ± 0.8	2.8 ± 0.7
4m	2.6 ± 0.8	28.8 ± 5.6	0.8 ± 0.09	0.23 ± 0.06	1.8 ± 0.6	1.6 ± 0.6
4n	11.1 ± 3.2	495 ± 24	43.3 ± 14.5	47.0 ± 0.06	66.2 ± 13.4	105 ± 47
4o	>10000	>10000	>10000	>10000	>10000	>10000
4p	6404 ± 1906	>10000	>10000	>10000	>10000	>10000
5a	952 ± 122	>10000	40.3 ± 16.6	209 ± 86	27.1 ± 8.2	265 ± 26
5b	0.3 ± 0.09	7.4 ± 2.2	0.7 ± 0.09	0.26 ± 0.08	2.8 ± 0.9	3.1 ± 1.2
3a	15 ± 4	100 ± 20	20 ± 3	5 ± 0.2	50 ± 9	n.d.
1	4 ± 1	180 ± 50	1 ± 0.2	5 ± 0.6	370 ± 100	3100 ± 100

[a] IC_{50} = compound concentration required to inhibit tumor cell proliferation by 50%. Data are expressed as the mean ± SE from the dose−response curves of at least three experiments.

Table 2. Inhibition of Tubulin Polymerization and Colchicine Binding by Compounds 1, 3a, 4e,f, 4i−n, and 5a,b

compd	tubulin assembly[a] IC_{50} ± SD (μM)	colchicine binding[b] % inhibition ± SD
4e	3.7 ± 0.5	47 ± 3
4f	2.5 ± 0.3	54 ± 0.3
4i	2.1 ± 0.2	60 ± 0.7
4j	3.5 ± 0.2	50 ± 1
4k	2.5 ± 0.1	59 ± 3
4l	1.1 ± 0.1	78 ± 3
4m	2.0 ± 0.2	58 ± 2
4n	3.1 ± 0.4	46 ± 4
5a	2.1 ± 0.3	70 ± 0.1
5b	2.0 ± 0.1	71 ± 2
3a	0.76 ± 0.1	86 ± 2
1	1.3 ± 0.1	99 ± 0.4

[a] Inhibition of tubulin polymerization. Tubulin was at 10 μM. [b] Inhibition of [^{3}H]colchicine binding. Tubulin, colchicine, and tested compound were at 1, 5, and 5 μM, respectively.

range of those of **1** and **3a** (IC_{50} of 1.3 and 0.76 μM, respectively). The remaining compounds were also good inhibitors of tubulin polymerization, with IC_{50} values ranging from 2 to 4 μM, so they were somewhat less active than **1** and **3a**.

While this group of compounds was highly potent in inhibition of cell growth and tubulin assembly, correlation between these two assays was imperfect, a finding that is frequently observed. Thus, compound **4l** was the best inhibitor of tubulin assembly, being 2-fold more potent than its isomeric derivative **5b** in this assay, but **4l** and **5b** were equipotent as inhibitors of cell growth.

In the colchicine binding studies, derivatives **4l** and **5a,b** had quantitatively similar effects, varying within a narrow range (70−78% inhibition), and they were slightly less potent than **1**, which in these experiments inhibited colchicine binding by 99%. For compounds **4e−f**, **4j−k**, and **4m,n**, inhibition of colchicine binding ranged from 46% to 58%, about half as active as **1** in this assay. In this series of 10 compounds, inhibition of [^{3}H]colchicine binding correlated more closely with inhibition of tubulin assembly than with antiproliferative activity.

Effects of 4l, 4m, and 5b on Drug Resistant Cell Lines. Drug resistance is an important therapeutic problem caused by the emergence of tumor cells possessing different mechanisms that confer resistance against a variety of anticancer drugs.[21,22] Among the more common mechanisms are those related to the overexpression of a cellular membrane protein called P-gp that mediates the efflux of various structurally unrelated drugs.[21,22] In this context, we evaluated sensitivity to the most active compounds (**4l**, **4m**, and **5b**) of two multidrug-resistant cell lines, one derived from a lymphoblastic leukemia ($CEM^{Vbl-100}$), the other derived from a colon carcinoma ($Lovo^{Doxo}$). Both these lines express high levels of the P-gp.[23,24] As shown in Table 3, the three compounds were equally potent toward parental cells and cells resistant to vinblastine or doxorubicin showing a resistance index, which is the ratio between IC_{50} values of resistant cells and sensitive cells, of about 1.

Resistance to microtubule inhibitors may also be mediated by changes in the levels of expression of different β-tubulin isotypes and by tubulin gene mutations that result in modified tubulin with impaired polymerization properties. A-549-T12 is a cell line with an α-tubulin mutation with increased resistance to paclitaxel.[25] Compounds **4l**, **4m**, and **5b** had greater relative activity than paclitaxel in this cell line, suggesting that these compounds might be useful in the treatment of drug refractory tumors resistant to other antitubulin drugs.

Molecular Modeling. Molecular docking simulations were performed on this series of compounds to understand the role

dx.doi.org/10.1021/jm2013979 | J. Med. Chem. 2012, 55, 475−488

Table 3. In Vitro Cell Growth Inhibitory Effects of Compounds on Drug Resistant Cell Lines

compd	IC_{50} [a] (nM) LoVo	$LoVo^{Doxo}$	resistance ratio [b]
4l	1.1 ± 0.9	0.7 ± 0.06	0.64
4m	12.5 ± 2.1	15.7 ± 6.5	1.3
5b	118.2 ± 60.5	96.9 ± 42.6	0.8
doxorubicin[c]	120 ± 30	13150 ± 210	109.6
	IC_{50} [a] (nM) CEM	CEM^{Vbl100}	resistance ratio [b]
4l	3.1 ± 1.0	0.7 ± 0.09	0.2
4m	0.7 ± 0.1	0.7 ± 0.2	1.0
5b	3.8 ± 1.4	0.5 ± 0.1	0.1
vinblastine[c]	4.1 ± 0.2	230 ± 32	56.1
	IC_{50} [a] (nM) A549	A549-T12	resistance ratio [b]
4l	8.1 ± 3.27	8.2 ± 5.0	1.0
4m	28.8 ± 5.6	31.5 ± 11.4	1.1
5b	7.4 ± 2.2	4.2 ± 1.8	0.6
paclitaxel[c]	7.2 ± 0.1	75.2 ± 12.5	10.4

[a] IC_{50} = compound concentration required to inhibit tumor cell proliferation by 50%. Data are expressed as the mean ± SE from the dose–response curves of at least three independent experiments. [b] The values express the ratio between IC_{50} values determined in resistant and nonresistant cell lines. [c] Data from ref 13c.

of the tetrazole ring in the binding interaction with tubulin, using the same procedures reported previously.[13c] Figure 1

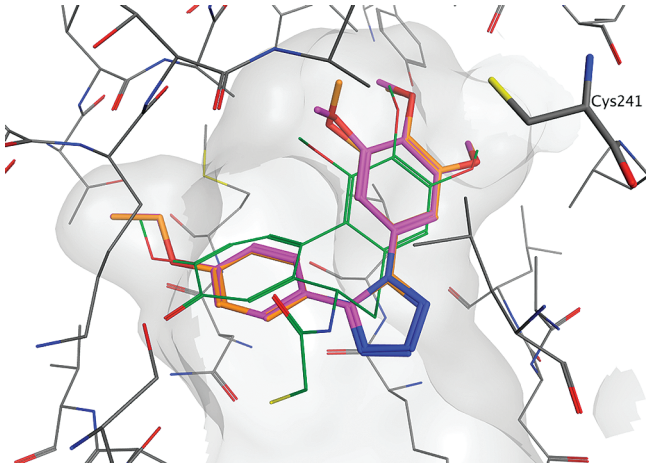

Figure 1. Proposed binding mode of **4l** (purple) and **5b** (orange) with DAMA-colchicine (green) in the β-tubulin binding site.

shows that the proposed binding of these compounds is very similar to the pose of the cocrystallized DAMA-colchicine, with the trimethoxyphenyl rings placed in proximity to βCys241 (amino acid residue numbers follow the modeling convention). Furthermore, the tetrazole is placed toward the external part of the pocket, and it does not seem to establish any specific interaction with tubulin. Indeed, the binding poses of the two isomers **4l** and **5b** are virtually identical. Another important consideration is that the binding modes of the tetrazole analogues were very similar to those observed for the triazole compounds **3a**,**b**.[13c] With the current compounds, only relatively small substituents were tolerated in the meta position of the second phenyl ring (e.g., **4i–k**), while analogues with larger groups, both in the meta and para positions (e.g., **4g–h** and **4o–p**) did not dock successfully, probably because of a steric clash with components of the binding pocket. These results correlate well with the biological data observed for these compounds.

Analysis of Cell Cycle Effects. The effects of different concentrations of compounds **4l**, **4m**, and **5b** after 24 h of treatment on cell cycle progression were examined in HeLa cells (Figure 2A). The two isomers **4l** and **5b** caused a significant G2/M arrest in a concentration-dependent manner, with a rise in G2/M cells occurring at a concentration as low as 30 nM, while at higher concentrations more than 80% of the cells were arrested in G2/M. This maximum was reached with the compounds at 60 nM. There was a concomitant decrease of cells in the other phases of the cell cycle (G1 and S). Treatment with compound **4m** produced similar G2/M arrest, but a somewhat higher concentration was required.

We next studied the association between **4l**-induced G2/M arrest and alterations in expression of proteins that regulate cell division. Cell arrest at the prometaphase/metaphase to anaphase transition is normally regulated by the mitotic checkpoint.[26] The major regulator of the G2 to M transition is M phase promoting factor (MPF), a complex made up of the catalytic subunit of cdc2 and the regulatory subunit of cyclin B. This and other regulatory complexes are activated at different points during the cell cycle and can also be regulated by several exogenous factors. Cyclin B/cdc2 complexes are held in an inactive state by phosphorylation of cdc2 at two negative regulatory sites (Thr14 and Tyr15). Dephosphorylation of these negative regulatory sites is needed to activate the cdc2/cyclin B complex. cdc25c is a major phosphatase that dephosphorylates both sites on cdc2 to activate its MPF activity.[27,28] As shown in Figure 2B in HeLa cells, **4l** caused a marked increase in cyclin B1 expression after both 24 and 48 h treatments. In addition, slower migrating forms of phosphatase cdc25c appeared at 24 h, indicating changes in the phosphorylation state of this protein, followed by an overall decrease in total cdc25c at 48 h. The phosphorylation of cdc25c directly stimulates its phosphatase activity, and this is necessary to activate cdc2/cyclin B on entry of cells into mitosis.[27,28] In addition, we observed dephosphorylation of cdc2 (Tyr15), particularly at 24 h, which should result in inhibition of formation of the cdc2/cyclinB complex.

Compounds 4l and 5b Induce Apoptosis. To characterize the mode of cell death induced by **4l** and **5b**, a biparametric cytofluorimetric analysis was performed using propidium iodide (PI), which stains DNA and enters only dead cells, and fluorescent immunolabeling of the protein annexin-V, which binds to phosphatidyl serine (PS) in a highly selective manner.[29] Dual staining for annexin-V and with PI permits discrimination between live cells (annexin-V^-/PI^-), early apoptotic cells (annexin-V^+/PI^-), late apoptotic cells (annexin-V^+/PI^+), and necrotic cells (annexin-V^-/PI^+) . As depicted in Figure 3, both compounds induced an accumulation of annexin-V positive cells in comparison with the control, in a concentration and time-dependent manner.

Effect of 4l and 5b on Mitochondrial Depolarization. Mitochondria play an essential role in the propagation of apoptosis.[30] It is well established that at an early stage, apoptotic stimuli alter the mitochondrial transmembrane potential ($\Delta\psi_{mt}$). $\Delta\psi_{mt}$ was monitored by the fluorescence of the dye 5,5′,6,6′-tetrachloro-1,1′,3,3′-tetraethylbenzimidazolcarbocyanine (JC-1). With normal cells (high $\Delta\psi_{mt}$), JC-1 displays

dx.doi.org/10.1021/jm2013979 | J. Med. Chem. 2012, 55, 475–488

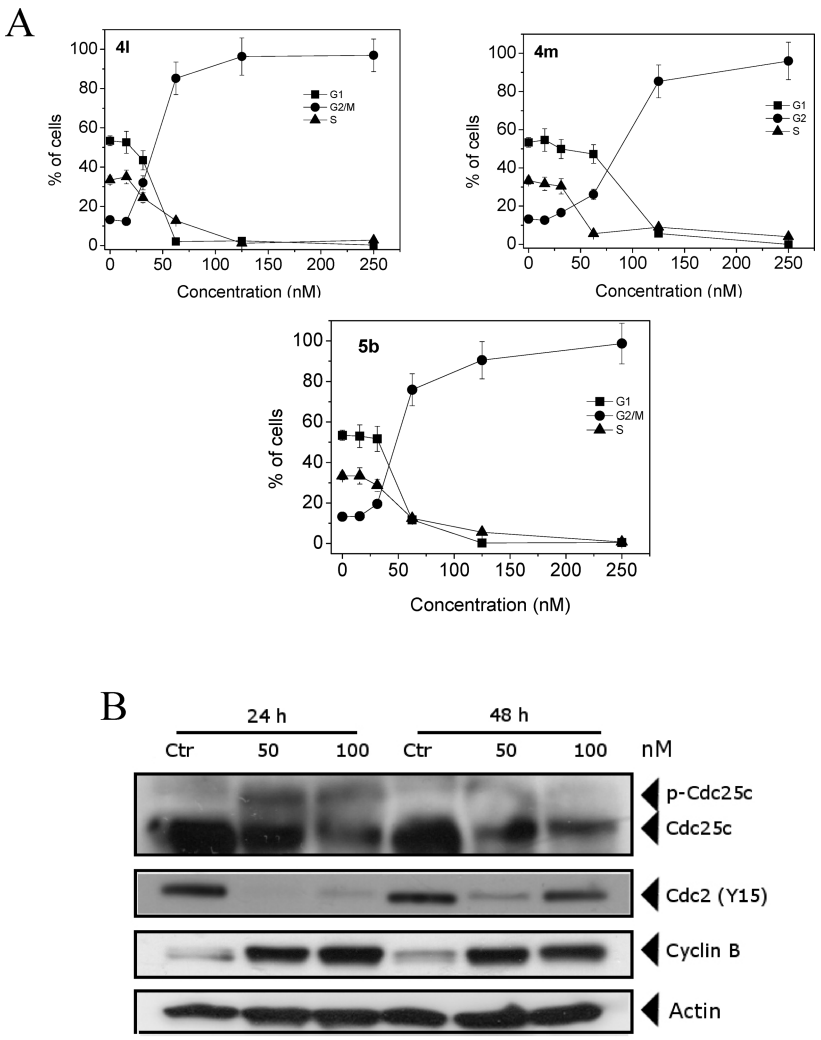

Figure 2. (A) Effect of compounds **4l**, **4m**, and **5b** on cell cycle distribution of HeLa cells. Cells were treated with different concentrations of the indicated compounds, ranging from 15 to 250 nM for 24 h. Then the cells were fixed and stained with PI to analyze DNA content by flow cytometry. Data are presented as the mean ± SEM of three independent experiments. (B) Effect of **4l** on G2/M regulatory proteins. HeLa cells were treated for 24 or 48 h with the indicated concentration of **4l**. The cells were harvested and lysed for the detection of cyclin B, p-cdc2^{Y15}, and cdc25c expression by Western blot analysis. To confirm equal protein loading, each membrane was stripped and reprobed with anti-β-actin antibody.

a red fluorescence (590 nm). This is caused by spontaneous and local formation of aggregates that are associated with a large shift in the emission. In contrast, when the mitochondrial membrane is depolarized (low $\Delta\psi_{mt}$), JC-1 forms monomers that emit at 530 nm. As shown in Figure 4, both **4l** and **5b** induced a time and concentration-dependent increase in the proportion of cells with depolarized mitochondria.

Mitochondrial membrane depolarization is associated with mitochondrial production of ROS.[31] Therefore, we investigated whether ROS production increased after treatment with **4l** and **5b**. We utilized two fluorescence indicators: hydroethydine (HE), whose fluorescence appears if ROS are generated,[32] and the dye 2,7-dichlorodihydrofluorescein diacetate (H_2-DCFDA), which is oxidized to the fluorescent compound dichlorofluorescein (DCF) by a variety of peroxides, including hydrogen peroxide.[32]

The results presented in Figure 5 (panels B and C) show that both **4l** and **5b** induced the production of significant amounts of ROS in comparison with control cells, which agrees with the previously described dissipation of $\Delta\psi_{mt}$. Altogether, these results indicate that these compounds induced apoptosis through the mitochondrial pathway. In this context, triazole derivative **3a** also induces apoptosis through the intrinsic pathway.[13c]

Compound 4l Induces Caspases Activation. Caspases, which are proteolytic enzymes, are the central executioners of apoptosis, and their activation is mediated by various inducers.[33] Synthesized as proenzymes, caspases are themselves activated by specific proteolytic cleavage reactions. Caspase-2, -8, -9, and -10 are termed apical caspases and are usually the first to be activated in the apoptotic process. Following their activation, they in turn activate effector caspases, in particular caspase-3.[34] Following treatment of HeLa cells with compound **4l** for 24 or 48 h, we observed activation of caspase-3 and of the caspase-3 substrate poly ADP-ribose polymerase (PARP) (Figure 6A). In addition, the expression of X-linked inhibitor of apoptosis protein (XIAP), a member of the apoptosis inhibitors protein family, was strongly reduced concomitant with caspase activation (Figure 6B). Consistent with the $\Delta\psi_{mt}$ results described above, **4l** treatment induced activation of caspase-9, the major initiator caspase of the intrinsic (mitochondrial) apoptosis pathway (Figure 6A).

dx.doi.org/10.1021/jm2013979 | J. Med. Chem. 2012, 55, 475−488

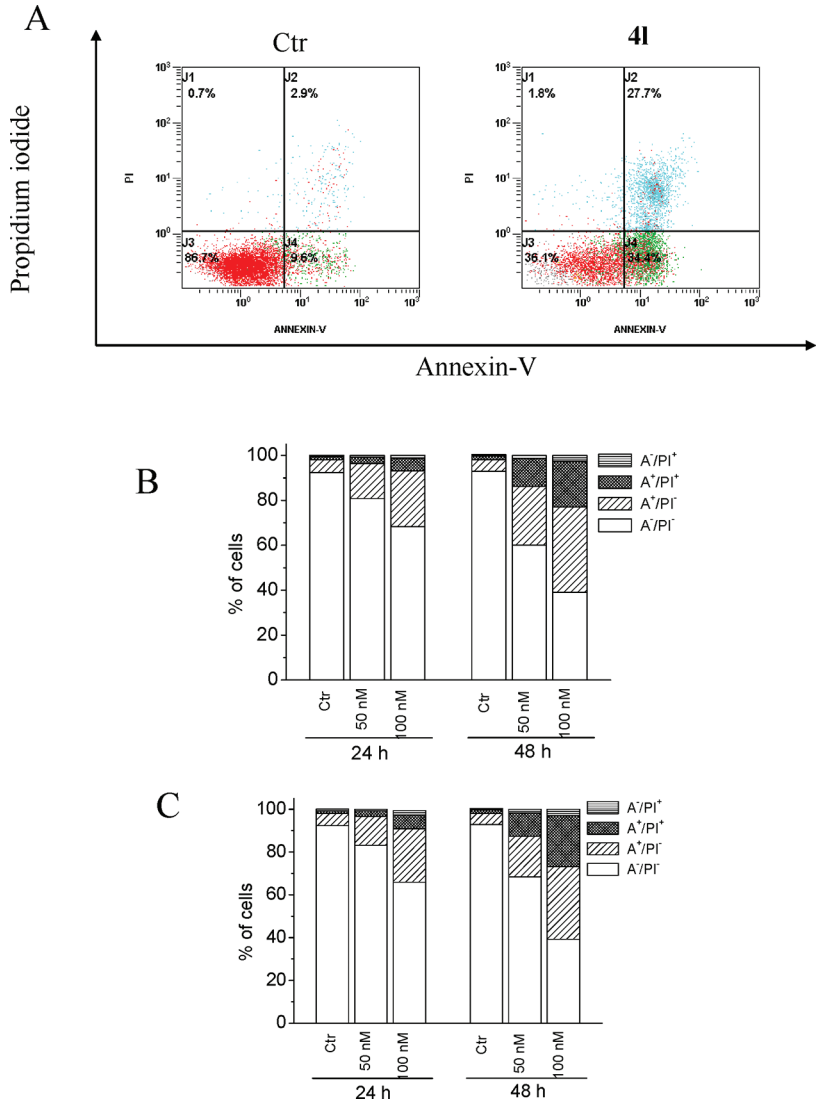

Figure 3. (A) Representative histograms of HeLa cells treated with **4l** (100 nM) for 48 h and analyzed by flow cytometry after double staining of the cells with annexin-V-FITC and PI. (B, C) Percentage of cells found in the different regions of the biparametric histograms obtained from cytofluorimetric analysis, after incubation with **4l** (B) or **5b** (C) for 24 or 48 h, as indicated.

We also examined whether the induction of apoptosis by **4l** was associated with changes in the expression of two proteins of the Bcl-2 family, since there is increasing evidence that they share the signaling pathways induced by antimicrotubule compounds.[35] However, our results showed (Figure 6B) that the antiapoptotic protein Bcl-2 was only slightly affected after 48 h of treatment, whereas **4l** treatment had no effect on the expression of the proapoptotic protein Bax.

In Vivo Antitumor Activity of Compound 4l. To evaluate the in vivo antitumor activity of **4l**, human colon adenocarcinoma xenografts were established by subcutaneous injection of HT29 cells in the backs of nude mice. Once the HT-29 xenografts reached a size of ~300 mm^3, 18 mice were randomly assigned to one of the three groups. In two of the groups, compound **4l** or reference compound **1**, dissolved in DMSO, was injected intraperitoneally at a dose of 100 mg/kg. Both drugs, as well as the vehicle control, were administered 3 times a week for 1 week. As shown in Figure 7 A, compound **4l** immediately caused a remarkable reduction in tumor growth, and this reached a 66% reduction by the end of the observation period compared with administration of vehicle only. The reduction in tumor growth was statistically significant as early as the day after the third dose of **4l**, suggesting a rapid, effective delivery of compound to the tumor mass. It is interesting to note that the effect on tumor volume reduction by **4l** was better than that of **1**, which caused a 43.7% of reduction at day 24.

During the whole treatment period, no significant weight changes occurred in the treated animals (Figure 7B), suggesting that **4l** has minimal toxicity.

■ CONCLUSIONS

We demonstrated that the 1,2,3,4-tetrazole ring is a suitable mimic for the cis-olefinic configuration present in **1**. *N*-1-(3′,4′,5′-Trimethoxyphenyl)tetrazole was the key intermediate for the preparation of many active compounds via a parallel synthesis. The observed antiproliferative activities depended on the substitution pattern on the phenyl at the 5-position of the tetrazole ring. The methoxy and ethoxy groups at the para-position, especially the latter, enhanced biological activity. The introduction of an additional EWG, such as F or Cl, or weak ERG (Me) group at the meta-position of this 4′-methoxy phenyl ring led to little change or further increased

dx.doi.org/10.1021/jm2013979 | J. Med. Chem. 2012, 55, 475−488

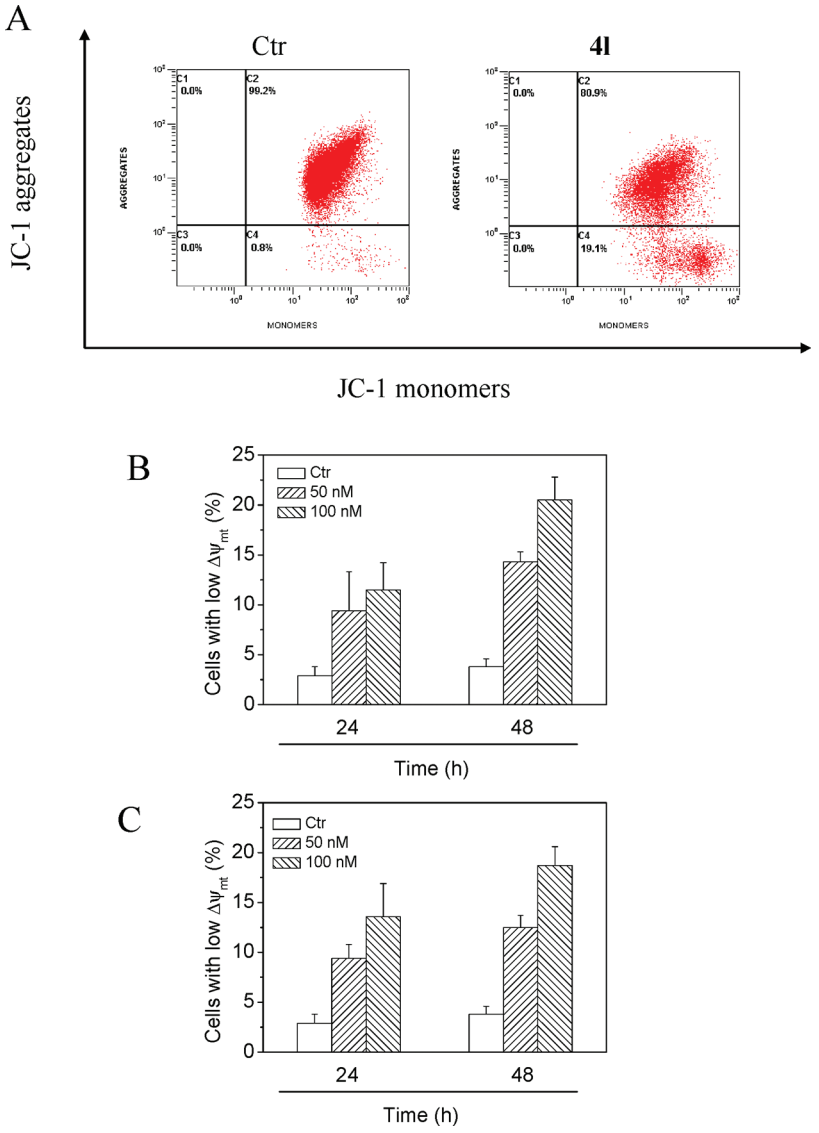

Figure 4. Assessment of $\Delta\psi_{mt}$ after treatment of HeLa cells with compounds **4l** and **5b**. (A) Representative histograms of both control cells and cells incubated 48 h in the presence of **4l**, as indicated, and stained with the fluorescent probe JC-1 after treatment. The horizontal axis shows fluorescence intensity of the JC-1 monomer, and the vertical axis shows fluorescence of JC-1 aggregates. (B, C). Induction of loss of mitochondrial membrane potential after 24 or 48 h incubations with compound **4l** (B) or **5b** (C). Data are expressed as the mean ± SEM of three independent experiments.

antiproliferative activity, but a *m*-methoxy group caused significant decrease in potency. The *p*-ethoxyphenyl derivative **4l** and its isomeric derivative **5b** had antiproliferative activities with IC_{50} values below 10 nM (0.3−8.1 nM). Replacement of the *p*-ethoxy group with larger alkoxy groups was detrimental for antiproliferative activity. These results imply that the 3′-hydroxy-4′-methoxyphenyl moiety of **1** (B-ring) can be replaced by a 4′-ethoxyphenyl group. Compound **4l** was a strong inhibitor of tubulin polymerization (IC_{50} = 1.1 μM) and strongly inhibited the binding of colchicine to tubulin (78% inhibition), with activities not greatly different from those of **1**.

We also showed that the tetrazole system that characterizes compound **4l** retained, or even improved on, the biological activity of the 1,2,4-triazole analogue **3a** previously reported. The 3′-chloro-4′-ethoxyphenyl derivative **4m** and the two isomeric 4′-ethoxyphenyl derivatives **4l** and **5b** were shown to arrest the cell cycle at the G2/M phase and induce apoptosis through the mitochondrial (intrinsic) pathway. Importantly, the antitumor efficacy of **4l** was demonstrated in a xenograft-bearing mouse. In this model, there was significant inhibition of tumor growth with only three doses of **4l**, and the treated animals had no significant weight loss. Our results demonstrated that **4l** is a promising new tubulin binding agent and is worthy of further evaluation as potential chemotherapeutic agent.

■ EXPERIMENTAL SECTION

Chemistry. Materials and Methods. ^{1}H NMR spectra were recorded on a Bruker AC 200 spectrometer. Chemical shifts (δ) are given in ppm upfield from tetramethylsilane as internal standard, and the spectra were recorded in appropriate deuterated solvents, as indicated. Positive-ion electrospray ionization (ESI) mass spectra were recorded on a double-focusing Finnigan MAT 95 instrument with BE geometry. Melting points (mp) were determined on a Buchi-Tottoli apparatus and are uncorrected. All products reported showed ^{1}H NMR spectra in agreement with the assigned structures. The purity of tested compounds was determined by combustion elemental analyses conducted by the Microanalytical Laboratory of the Department of Chemistry of the University of Ferrara, Italy, with a Yanagimoto MT-5

dx.doi.org/10.1021/jm2013979 | J. Med. Chem. 2012, 55, 475−488

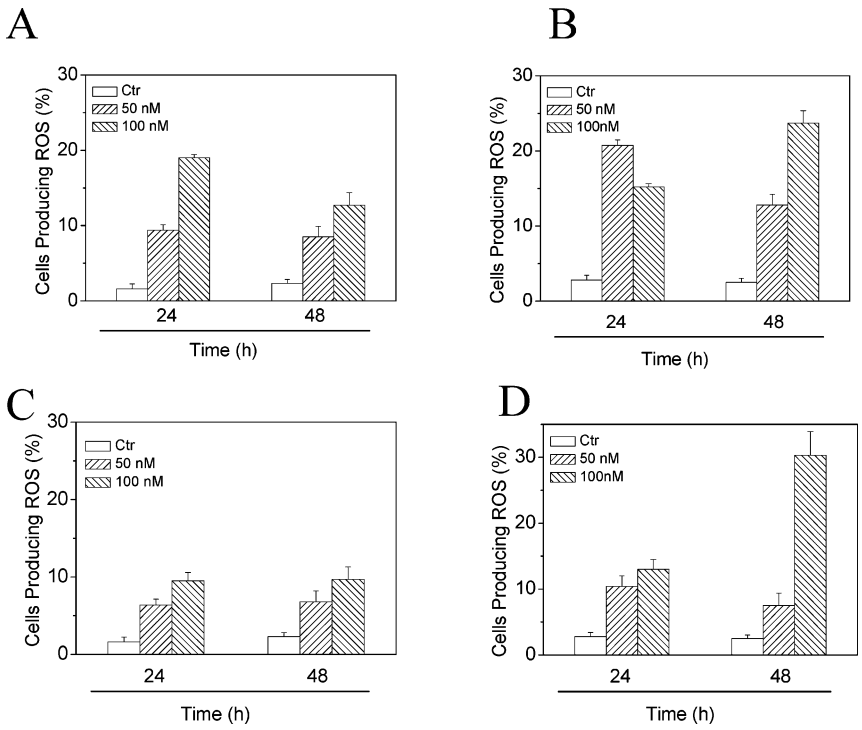

Figure 5. Mitochondrial production of ROS in HeLa cells following treatment with compound **4l** (A, B) or compound **5b** (C, D). After the 24 or 48 h incubations, cells were stained with HE (A, C) or H_2-DCFDA (B, D) and analyzed by flow cytometry. Data are expressed as the mean ± SEM of three independent experiments.

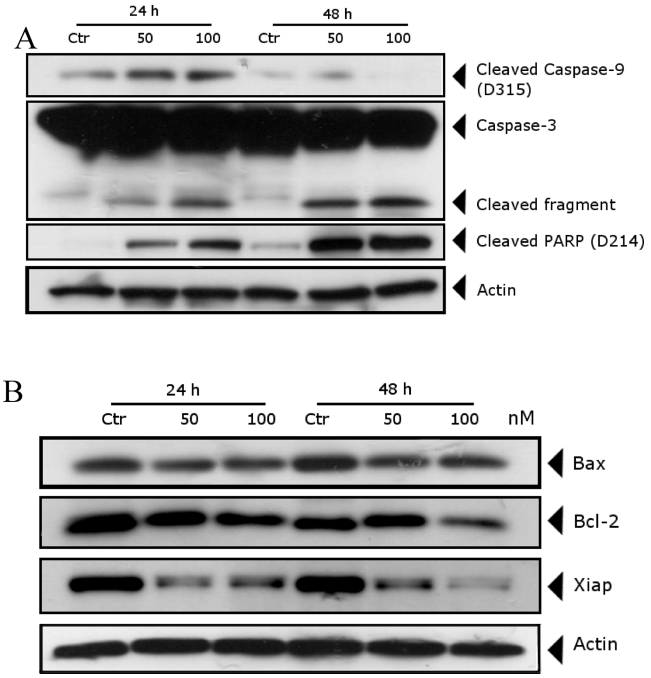

Figure 6. (A) Western blot analysis of caspase-3, cleaved caspase-9, and cleaved PARP after treatment of HeLa cells with **4l** at the indicated concentration and for the indicated times. (B) Western blot analysis of Bcl-2, Bax, and XIAP after treatment of HeLa cells with **4l** at the indicated concentration and for the indicated times. To confirm equal protein loading, each membrane was stripped and reprobed with anti-β-actin antibody.

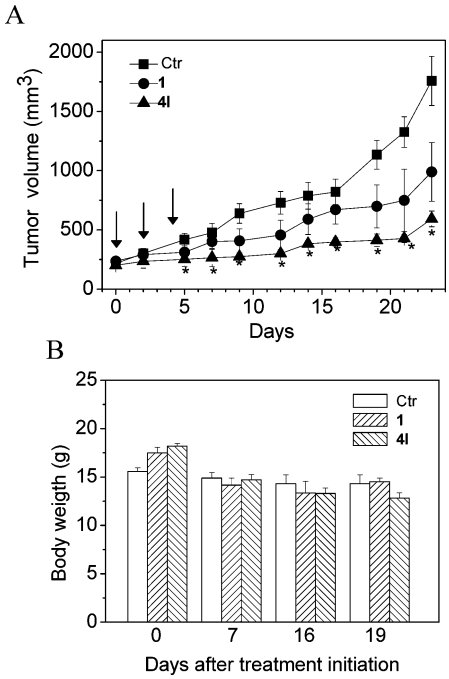

Figure 7. Inhibition of human xenograft growth in vivo by compound **4l**. (A) HT29 tumor-bearing nude mice were administered the vehicle, as control, or 100 mg/kg **4l** or **1**. Injections were given intraperitoneally on days 0, 2, and 4 (indicated by arrows). The figure shows the average measured tumor volumes (A) and body weights of the mice (B) recorded on the indicated days after treatments. Data are expressed as the mean ± SEM of tumor volume and body weight at each time point for six animals per group: *, $p < 0.01$ vs control.

CHN recorder elemental analyzer. All tested compounds yielded data consistent with a purity of at least 95% compared with the theoretical values. All reactions were carried out under an inert atmosphere of dry nitrogen, unless otherwise indicated. Standard syringe techniques were used for transferring dry solvents. Reaction courses and product

dx.doi.org/10.1021/jm2013979 | J. Med. Chem. 2012, 55, 475–488

mixtures were routinely monitored by TLC on silica gel (precoated F_{254} Merck plates), and compounds were visualized with aqueous $KMnO_4$. Flash chromatography was performed using 230−400 mesh silica gel and the indicated solvent system. Organic solutions were dried over anhydrous Na_2SO_4. Anilines **6a−c**, aryl iodides, and arylboronic acids are commercially available and used as received. The synthesis of 4-pentyloxyiodobenzene was performed as previously described.:[36]

General Procedure A for the Synthesis of 1-Aryl Substituted 1*H*-Tetrazoles 7a−c. A stirred suspension of the appropriate aniline **6a−c** (14 mmol), triethyl orthoformate (3.7 mL, 22.5 mmol), and sodium azide (1.36 g., 21 mmol) in acetic acid (15 mL) was refluxed for 4 h. The mixture was cooled, the solvent was removed in vacuo and the residue dissolved in a mixture of dichloromethane (50 mL) and 0.1 N aqueous HCl (20 mL). The organic phase was washed with water (20 mL), brine (10 mL), dried over Na_2SO_4, and concentrated. The residue was suspended in ethyl ether (15 mL), stirred for 30 min, and filtered to afford the desired product.

1-(3,4,5-Trimethoxyphenyl)-1*H*-tetrazole (7c). Following general procedure A, compound **6c** was isolated as a gray solid (yield >95%), mp 172−173 °C. ^{1}H NMR ($CDCl_3$) δ: 3.89 (s, 6H), 3.93 (s, 3H), 6.89 (s, 2H), 8.96 (s, 1H).

General Procedure B for the Synthesis of 5-Bromo-1-aryl Substituted 1*H*-Tetrazoles 8a−c. To a suspension of the appropriate 1-aryl substituted tetrazole **7a−c** (10 mmol) in carbon tetrachloride (100 mL) heated at reflux were added *N*-bromosuccinimide (3.56 g., 20 mmol) and benzoyl peroxide (120 mg, 5 mmol). The reflux continued for 4 h, and another portion of benzoyl peroxide was added to the mixture (120 mg, 5 mmol). After 18 h, the solution was diluted with dichloromethane (100 mL) and subsequently washed with 5% aqueous $Na_2S_2O_3$ (50 mL), water (50 mL), brine (50 mL), dried (Na_2SO_4), and concentrated. The residue was purified by column chromatography on silica gel using the indicated eluent mixture to afford the desired product.

5-Bromo-1-(4-methoxyphenyl)-1*H*-tetrazole (8a). Following general procedure B, starting from 1-(4-methoxyphenyl)-1*H*-tetrazole **7a**, the crude residue was purified by column chromatography on silica gel (petroleum ether−ethyl acetate, 2:8) to afford **8a** as a yellow solid. Yield 49%, mp 110−111 °C. ^{1}H NMR ($CDCl_3$) δ: 3.90 (s, 3H), 7.06 (d, J = 9.0 Hz, 2H), 7.45 (d, J = 9.0 Hz, 2H).

5-Bromo-1-(4-ethoxyphenyl)-1*H*-tetrazole (8b). Following general procedure B, starting from 1-(4-ethoxyphenyl)-1*H*-tetrazole **7b**, the crude residue was purified by column chromatography on silica gel (petroleum ether−ethyl acetate, 2:8) to afford **8b** as a gray solid. Yield 70%, mp 116−117 °C. ^{1}H NMR ($CDCl_3$) δ: 1.47 (t, J = 6.8 Hz, 3H), 4.13 (q, J = 6.8 Hz, 2H), 7.04 (dd, J = 8.6 and 2.2 Hz, 2H), 7.44 (dd, J = 8.6 and 2.2 Hz, 2H).

5-Bromo-1-(3,4,5-trimethoxyphenyl)-1*H*-tetrazole (8c). Following general procedure B, starting from 1-(3,4,5-trimethoxyphenyl)-1*H*-tetrazole **7c**, the crude residue was purified by column chromatography on silica gel (petroleum ether−ethyl acetate, 3:7) to afford **8c** as a brown solid. Yield 24%, mp 130−131 °C. ^{1}H NMR ($CDCl_3$) δ: 3.91 (s, 6H), 3.92 (s, 3H), 6.74 (s, 2H).

General Procedure C for the Arylation of 5-Bromo-1-aryl Substituted 1*H*-Tetrazoles 8a−c. A solution of 5-bromo-1-aryl substituted 1*H*-tetrazole **8a−c** (0.5 mmol), the appropriate arylboronic acid (1 mmol, 2 equiv), and 2 M aqueous Na_2CO_3 (0.5 mL) in a mixture of toluene (5 mL) and ethanol (0.5 mL) was purged with nitrogen for 5 min. Tetrakis(triphenylphosphine)palladium (54 mg, 0.05 mmol) was added and the mixture heated with stirring at 120 °C under argon for 18 h. After this time, the suspension was cooled to ambient temperature, diluted with dichloromethane (10 mL), and filtered through a pad of Celite, and the filtrate was evaporated in vacuo. The residue was dissolved with dichloromethane (20 mL), and the resultant solution was washed sequentially with 2 M aqueous Na_2CO_3 (10 mL), water (10 mL), and brine (10 mL). The organic layer was dried, filtered, and evaporated, and the residue was purified by flash chromatography on silica gel, using a mixture of ethyl acetate−petroleum ether as eluent.

General Procedure D for the Direct Arylation of 1-(3,4,5-Trimethoxyphenyl)-1*H*-tetrazole (7c). A suspension of 1-(3,4,5-trimethoxyphenyl)-1*H*-tetrazole **7c** (236 mg, 1.00 mmol), the appropriate aryl iodide (1.00 mmol), cesium carbonate (358 mg, 1.1 mmol), copper(I) iodide (190 mg, 1 mmol), palladium(II) acetate (11.2 mg, 0.05 mmol), and TFP (23.2 mg, 0.1 mmol) in dry acetonitrile (5 mL) was heated under argon for 6 h at 45 °C. The resulting mixture was diluted with dichloromethane (10 mL) and filtered through Celite, and the solvents were removed under reduced pressure. The residue was dissolved in a mixture of dichloromethane (15 mL) and 0.1 N aqueous HCl (5 mL). The organic phase was washed with water (5 mL) and brine (5 mL), dried over Na_2SO_4, and concentrated under reduced pressure. The residue was purified by column chromatography on silica gel (mixture of petroleum ether−ethyl acetate as eluent) to afford the title compound.

1-(3,4,5-Trimethoxyphenyl)-5-phenyl-1*H*-tetrazole (4a). Following general procedure D, the crude residue was purified by flash chromatography, using ethyl acetate−petroleum ether, 2:8 (v/v), as eluent, to furnish **4a** as a brown solid (48% yield), mp 148−149 °C. ^{1}H NMR ($CDCl_3$) δ: 3.76 (s, 6H), 3.91 (s, 3H), 6.59 (s, 2H), 7.46 (m, 3H), 7.64 (m, 2H). MS (ESI): $[M]^+$ = 312.6. Anal. ($C_{16}H_{16}N_4O_3$) C, H, N.

1-(3,4,5-Trimethoxyphenyl)-5-(thiophen-2-yl)-1*H*-tetrazole (4b). Following general procedure D, the crude residue was purified by flash chromatography, using ethyl acetate−petroleum ether, 3:7 (v.v), as eluent to furnish **4b** as a pale brown solid (54% yield), mp 197−199 °C. ^{1}H NMR ($CDCl_3$) δ: 3.84 (s, 6H), 3.95 (s, 3H), 6.67 (s, 2H), 7.08 (dd, J = 5.2 and 4.0 Hz, 1H), 7.39 (dd, J = 3.6 and 1.0 Hz, 1H), 7.54 (dd, J = 5.2 and 1.6 Hz, 1H). MS (ESI): $[M]^+$ = 318.6. Anal. ($C_{14}H_{14}N_4SO_3$) C, H, N.

1-(4-(1-(3,4,5-Trimethoxyphenyl)-1*H*-tetrazol-5-yl)phenyl)-ethanone (4c). Following general procedure D, the crude residue was purified by flash chromatography, using ethyl acetate−petroleum ether, 4:6 (v/v), as eluent, to furnish **4c** as a pale brown solid (62% yield), mp 146−147 °C. ^{1}H NMR ($CDCl_3$) δ: 2.63 (s, 3H), 3.77 (s, 6H), 3.92 (s, 3H), 6.58 (s, 2H), 7.76 (d, J = 8.8 Hz, 2H), 7.98 (d, J = 8.8 Hz, 2H). MS (ESI): $[M]^+$ = 354.8. Anal. ($C_{18}H_{18}N_4O_4$) C, H, N.

1-(3,4,5-Trimethoxyphenyl)-5-*p*-tolyl-1*H*-tetrazole (4d). Following general procedure C, the crude residue was purified by flash chromatography, using ethyl acetate−petroleum ether, 3:7 (v/v), as eluent, to furnish **4d** as a pale brown solid (56% yield), mp 98−100 °C. ^{1}H NMR ($CDCl_3$) δ: 2.39 (s, 3H), 3.77 (s, 6H), 3.92 (s, 3H), 6.59 (s, 2H), 7.21 (d, J = 8.2 Hz, 2H), 7.51 (d, J = 8.2 Hz, 2H). MS (ESI): $[M]^+$ = 326.8. Anal. ($C_{17}H_{18}N_4O_3$) C, H, N.

1-(3,4,5-Trimethoxyphenyl)-5-(4-ethylphenyl)-1*H*-tetrazole (4e). Following general procedure D, the crude residue was purified by flash chromatography, using ethyl acetate−petroleum ether, 3:7 (v/v), as eluent, to furnish **4e** as a pale brown solid (52% yield), mp 156−157 °C. ^{1}H NMR ($CDCl_3$) δ: 1.24 (t, J = 7.6 Hz, 3H), 2.71 (q, J = 7.6 Hz, 2H), 3.76 (s, 6H), 3.91 (s, 3H), 6.59 (s, 2H), 7.23 (d, J = 8.6 Hz, 2H), 7.55 (d, J = 8.6 Hz, 2H). MS (ESI): $[M]^+$ = 340.7. Anal. ($C_{18}H_{20}N_4O_3$) C, H, N.

1-(3,4,5-Trimethoxyphenyl)-5-(4-methoxyphenyl)-1*H*-tetrazole (4f). Following general procedure D, the crude residue was purified by flash chromatography, using ethyl acetate−petroleum ether, 3:7 (v/v), as eluent, to furnish **4f** as a yellow solid (49% yield), mp 144−145 °C. ^{1}H NMR ($CDCl_3$) δ: 3.78 (s, 3H), 3.84 (s, 3H), 3.86 (s, 3H), 3.92 (s, 3H), 6.60 (s, 2H), 6.91 (d, J = 9.0 Hz, 2H), 7.56 (d, J = 9.0 Hz, 2H). MS (ESI): $[M]^+$ = 342.9. Anal. ($C_{17}H_{18}N_4O_4$) C, H, N.

1-(3,4,5-Trimethoxyphenyl)-5-(3,4-dimethoxyphenyl)-1*H*-tetrazole (4g). Following general procedure D, the crude residue was purified by flash chromatography, using ethyl acetate−petroleum ether, 4:6 (v/v), as eluent, to furnish **4g** as a pale brown solid (54% yield), mp 158−159 °C. ^{1}H NMR ($CDCl_3$) δ: 3.78 (s, 6H), 3.82 (s, 3H), 3.84 (s, 3H), 3.91 (s, 3H), 6.63 (s, 2H), 6.83 (d, J = 8.6 Hz, 1H), 7.02 (dd, J = 8.6 and 2.0 Hz, 1H), 7.30 (d, J = 2.0 Hz, 1H). MS (ESI): $[M]^+$ = 372.9. Anal. ($C_{18}H_{20}N_4O_5$) C, H, N.

1,5-Bis(3,4,5-trimethoxyphenyl)-1*H*-tetrazole (4h). Following general procedure D, the crude residue was purified by flash

dx.doi.org/10.1021/jm2013979 | *J. Med. Chem.* 2012, 55, 475−488

chromatography, using ethyl acetate−petroleum ether, 4:6 (v/v), as eluent, to furnish **4h** as a white solid (56% yield), mp 135−136 °C. ^{1}H NMR ($CDCl_3$) δ: 3.71 (s, 6H), 3.81 (s, 3H), 3.85 (s, 3H), 3.88 (s, 3H), 3.90 (s, 3H), 6.65 (s, 2H), 6.87 (s, 2H). MS (ESI): $[M]^+$ = 402.9. Anal. ($C_{19}H_{22}N_4O_6$) C, H, N.

5-(3-Fluoro-4-methoxyphenyl)-1-(3,4,5-trimethoxyphenyl)-1*H*-tetrazole (4i). Following general procedure C, the crude residue was purified by flash chromatography, using ethyl acetate−petroleum ether, 4:6 (v/v), as eluent, to furnish **4i** as a pale brown solid (49% yield), mp 171−172 °C. ^{1}H NMR ($CDCl_3$) δ: 3.79 (s, 6H), 3.91 (s, 3H), 3.92 (s, 3H), 6.58 (s, 2H), 6.96 (t, J = 8.0 Hz, 1H), 7.37 (m, 2H). MS (ESI): $[M]^+$ = 360.4. Anal. ($C_{17}H_{17}FN_4O_4$) C, H, N.

5-(3-Chloro-4-methoxyphenyl)-1-(3,4,5-trimethoxyphenyl)-1*H*-tetrazole (4j). Following general procedure C, the crude residue was purified by flash chromatography, using ethyl acetate−petroleum ether, 3:7 (v/v), as eluent, to furnish **4j** as a yellow solid (52% yield), mp 175−177 °C. ^{1}H NMR ($CDCl_3$) δ: 3.80 (s, 6H), 3.92 (s, 3H), 3.94 (s, 3H), 6.61 (s, 2H), 6.91 (d, J = 8.6 Hz, 1H), 7.46 (dd, J = 8.4 and 2.2 Hz, 1H), 7.73 (d, J = 2.2 Hz, 1H). MS (ESI): $[M]^+$ = 376.8. Anal. ($C_{17}H_{17}ClN_4O_4$) C, H, N.

5-(3-Methyl-4-methoxyphenyl)-1-(3,4,5-trimethoxyphenyl)-1*H*-tetrazole (4k). Following general procedure C, the crude residue was purified by flash chromatography, using ethyl acetate−petroleum ether, 3:7 (v/v), as eluent, to furnish **4k** as a pale brown solid (51% yield), mp 152−153 °C. ^{1}H NMR ($CDCl_3$) δ: 2.19 (s, 3H), 3.78 (s, 6H), 3.84 (s, 3H), 3.92 (s, 3H), 6.62 (s, 2H), 6.79 (d, J = 8.6 Hz, 1H), 7.34 (dd, J = 8.6 and 1.4 Hz, 1H), 7.54 (d, J = 1.4 Hz, 1H). MS (ESI): $[M]^+$ = 356.8. Anal. ($C_{18}H_{20}N_4O_4$) C, H, N.

1-(3,4,5-Trimethoxyphenyl)-5-(4-ethoxyphenyl)-1*H*-tetrazole (4l). Following general procedure D, the crude residue was purified by flash chromatography, using ethyl acetate−petroleum ether, 3:7 (v/v), as eluent, to furnish **4l** as a pale brown solid (53% yield), mp 170−171 °C. ^{1}H NMR ($CDCl_3$) δ: 1.43 (t, J = 7.0 Hz, 3H), 3.78 (s, 6H), 3.92 (s, 3H), 4.07 (q, J = 7.0 Hz, 2H), 6.61 (s, 2H), 6.91 (d, J = 8.8 Hz, 2H), 7.54 (d, J = 8.8 Hz, 2H). MS (ESI): $[M]^+$ = 356.9. Anal. ($C_{18}H_{20}N_4O_4$) C, H, N.

5-(3-Chloro-4-ethoxyphenyl)-1-(3,4,5-trimethoxyphenyl)-1*H*-tetrazole (4m). Following general procedure C, the crude residue was purified by flash chromatography, using ethyl acetate−petroleum ether, 3:7 (v/v), as eluent, to furnish **4m** as a red solid (52% yield), mp 75−77 °C. ^{1}H NMR ($CDCl_3$) δ: 1.49 (t, J = 7.0 Hz, 3H), 3.80 (s, 6H), 3.92 (s, 3H), 4.13 (q, J = 7.0 Hz, 2H), 6.61 (s, 2H), 6.90 (d, J = 8.6 Hz, 1H), 7.39 (dd, J = 8.6 and 2.2 Hz, 1H), 7.76 (d, J = 2.2 Hz, 1H). MS (ESI): $[M]^+$ = 390.9. Anal. ($C_{18}H_{19}ClN_4O_4$) C, H, N.

1-(3,4,5-Trimethoxyphenyl)-5-(4-propoxyphenyl)-1*H*-tetrazole (4n). Following general procedure D, the crude residue was purified by flash chromatography, using ethyl acetate−petroleum ether, 3:7 (v/v), as eluent, to furnish **4n** as a yellow solid (49% yield), mp 152−154 °C. ^{1}H NMR ($CDCl_3$) δ: 1.04 (t, J = 7.2 Hz, 3H), 1.84 (m, 2H), 3.79 (s, 6H), 3.92 (s, 3H), 4.03 (q, J = 7.2 Hz, 2H), 6.61 (s, 2H), 6.92 (d, J = 9.0 Hz, 2H), 7.55 (d, J = 9.0 Hz, 2H). MS (ESI): $[M]^+$ = 370.8. Anal. ($C_{19}H_{22}N_4O_4$) C, H, N.

5-(4-Butoxyphenyl)-1-(3,4,5-trimethoxyphenyl)-1*H*-tetrazole (4o). Following general procedure D, the crude residue was purified by flash chromatography, using ethyl acetate−petroleum ether, 2:8 (v/v), as eluent, to furnish **4o** as a white solid (51% yield), mp 133−134 °C. ^{1}H NMR ($CDCl_3$) δ: 0.97 (t, J = 7.0 Hz, 3H), 1.52 (m, 2H), 1.84 (m, 2H), 3.78 (s, 6H), 3.92 (s, 3H), 3.98 (q, J = 7.0 Hz, 2H), 6.61 (s, 2H), 6.90 (d, J = 9.0 Hz, 2H), 7.55 (d, J = 9.0 Hz, 2H). MS (ESI): $[M]^+$ = 384.8. Anal. ($C_{20}H_{24}N_4O_4$) C, H, N.

1-(3,4,5-Trimethoxyphenyl)-5-(4-(pentyloxy)phenyl)-1*H*-tetrazole (4p). Following general procedure D, the crude residue was purified by flash chromatography, using ethyl acetate−petroleum ether, 3:7 (v/v), as eluent, to furnish **4p** as a pale brown solid (54% yield), mp 143−144 °C. ^{1}H NMR ($CDCl_3$) δ: 0.93 (t, J = 7.0 Hz, 3H), 1.44 (m, 4H), 1.82 (m, 2H), 3.78 (s, 6H), 3.92 (s, 3H), 3.97 (q, J = 7.0 Hz, 2H), 6.61 (s, 2H), 6.90 (d, J = 9.0 Hz, 2H), 7.55 (d, J = 9.0 Hz, 2H). $[M]^+$ = 398.9. Anal. ($C_{21}H_{26}N_4O_4$) C, H, N.

5-(3,4,5-Trimethoxyphenyl)-1-(4-methoxyphenyl)-1*H*-tetrazole (5a). Following general procedure C, the crude residue was purified by flash chromatography, using ethyl acetate−petroleum ether, 4:6 (v/v), as eluent, to furnish **5a** as a white solid (64% yield), mp 120−121 °C. ^{1}H NMR ($CDCl_3$) δ: 3.69 (s, 6H), 3.88 (s, 3H), 3.89 (s, 3H), 6.81 (s, 2H), 7.02 (d, J = 9.0 Hz, 2H), 7.34 (d, J = 9.0 Hz, 2H). MS (ESI): $[M]^+$ = 342.8. Anal. ($C_{17}H_{18}N_4O_4$) C, H, N.

5-(3,4,5-Trimethoxyphenyl)-1-(4-ethoxyphenyl)-1*H*-tetrazole (5b). Following general procedure C, the crude residue was purified by flash chromatography, using ethyl acetate−petroleum ether, 3:7 (v/v), as eluent, to furnish **5b** as a pale brown solid (54% yield), mp 94−95 °C. ^{1}H NMR ($CDCl_3$) δ: 1.41 (t, J = 6.8 Hz, 3H), 3.68 (s, 6H), 3.87 (s, 3H), 4.10 (q, J = 6.8 Hz, 2H), 6.81 (s, 2H), 7.00 (d, J = 8.8 Hz, 2H), 7.32 (d, J = 8.8 Hz, 2H). MS (ESI): $[M]^+$ = 356.9. Anal. ($C_{18}H_{20}N_4O_4$) C, H, N.

Biology. Materials and Methods. Antiproliferative Assays. Human T-leukemia (Jurkat) and human promyelocytic leukemia (HL-60) cells were grown in RPMI-1640 medium (Gibco, Milano, Italy). Breast adenocarcinoma (MCF7), human non-small-cell lung carcinoma (A549), human cervix carcinoma (HeLa), and human colon adenocarcinoma (HT-29) cells were grown in DMEM medium (Gibco, Milano, Italy), all supplemented with 115 units/mL penicillin G (Gibco, Milano, Italy), 115 μg/mL streptomycin (Invitrogen, Milano, Italy), and 10% fetal bovine serum (Invitrogen, Milano, Italy). LoVo^{Doxo} cells are a doxorubicin resistant subclone of LoVo cells[22] and were grown in complete Ham's F12 medium supplemented with doxorubicin (0.1 μg/mL). CEM$^{Vbl\text{-}100}$ are a multidrug-resistant line selected against vinblastine.[23] A549-T12 are non-small-cell lung carcinoma cells exhibiting resistance to paclitaxel.[24] They were grown in complete DMEM medium supplemented with paclitaxel (12 nM). Stock solutions (10 mM) of the different compounds were obtained by dissolving them in DMSO. Individual wells of a 96-well tissue culture microtiter plate were inoculated with 100 μL of complete medium containing 8×10^3 cells. The plates were incubated at 37 °C in a humidified 5% CO_2 incubator for 18 h prior to the experiments. After medium removal, 100 μL of fresh medium containing the test compound at different concentrations was added to each well and incubated at 37 °C for 72 h. The percentage of DMSO in the medium never exceeded 0.25%. This was also the maximum DMSO concentration in all cell-based assays described below. Cell viability was assayed by the (3-(4,5-dimethylthiazol-2-yl)-2,5-diphenyltetrazolium bromide test as previously described.[37] The IC_{50} was defined as the compound concentration required to inhibit cell proliferation by 50%, in comparison to cells treated with the maximum amount of DMSO (0.25%) and considered as 100% viability.

Effects on Tubulin Polymerization and on Colchicine Binding to Tubulin. To evaluate the effect of the compounds on tubulin assembly in vitro,[20a] varying concentrations of compounds were preincubated with 10 μM bovine brain tubulin in glutamate buffer at 30 °C and then cooled to 0 °C. After addition of 0.4 mM GTP, the mixtures were transferred to 0 °C cuvettes in a recording spectrophotometer and warmed to 30 °C. Tubulin assembly was followed turbidimetrically at 350 nm. The IC_{50} was defined as the compound concentration that inhibited the extent of assembly by 50% after a 20 min incubation. The capacity of the test compounds to inhibit colchicine binding to tubulin was measured as described[20b] except that the reaction mixtures contained 1 μM tubulin, 5 μM [^{3}H]colchicine, and 5 μM test compound.

Molecular Modeling. All molecular modeling studies were performed on a MacPro dual 2.66 GHz Xeon running Ubuntu 8. The tubulin structure was downloaded from the PDB (http://www.rcsb.org/, PDB code 1SA0).[38] Hydrogen atoms were added to the protein, using Molecular Operating Environment (MOE),[39] and minimized keeping all the heavy atoms fixed until a rmsd gradient of 0.05 kcal mol^{-1} Å^{-1} was reached. Ligand structures were built with MOE and minimized using the MMFF94x force field until a rmsd gradient of 0.05 kcal mol^{-1} Å^{-1} was reached. The docking simulations were performed using PLANTS.[40]

Flow Cytometric Analysis of Cell Cycle Distribution. For flow cytometric analysis of DNA content, 5×10^5 HeLa cells in exponential growth were treated with different concentrations of the test compounds for 24 and 48 h. After the incubation period, the cells were collected, centrifuged, and fixed with ice-cold ethanol (70%). The

dx.doi.org/10.1021/jm2013979 | J. Med. Chem. 2012, 55, 475−488

cells were then treated with lysis buffer containing RNase A and 0.1% Triton X-100 and then stained with PI. Samples were analyzed on a Cytomic FC500 flow cytometer (Beckman Coulter). DNA histograms were analyzed using MultiCycle for Windows (Phoenix Flow Systems).

Annexin-V Assay. Surface exposure of PS on apoptotic cells was measured by flow cytometry with a Coulter Cytomics FC500 (Beckman Coulter) by adding annexin-V-FITC to cells according to the manufacturer's instructions (Annexin-V Fluos, Roche Diagnostics). Simultaneously, the cells were stained with PI. Excitation was set at 488 nm, and the emission filters were at 525 and 585 nm, respectively, for FTIC and PI.

Assessment of Mitochondrial Changes. The mitochondrial membrane potential was measured with the lipophilic cationic dye JC-1 (Molecular Probes), as described.[13c] The production of ROS was measured by flow cytometry using either HE (Molecular Probes) or H_2DCFDA (Molecular Probes), as previously described.[13c]

Western Blot Analysis. HeLa cells were incubated in the presence of test compounds and, after different times, were collected, centrifuged, and washed two times with ice cold phosphate buffered saline (PBS). The pellet was then resuspended in lysis buffer. After the cells were lysed on ice for 30 min, lysates were centrifuged at 15000*g* at 4 °C for 10 min. The protein concentration in the supernatant was determined using the BCA protein assay reagents (Pierce, Italy). Equal amounts of protein (20 μg) were resolved using sodium dodecyl sulfate−polyacrylamide gel electrophoresis (SDS−PAGE) (7.5−15% acrylamide gels) and transferred to PVDF Hybond-P membrane (GE Healthcare). Membranes were blocked with I-Block (Tropix), the membrane being gently rotated overnight at 4 °C. Membranes were then incubated with primary antibodies against Bcl-2, Bax, cleaved PARP, cleaved caspase-9, p-cdc2^{Tyr15}, cdc25c (Cell Signaling), caspase-3 (Alexis), cyclin B (Upstate), or β-actin (Sigma-Aldrich) for 2 h at room temperature. Membranes were next incubated with peroxidase-labeled secondary antibodies for 60 min. All membranes were visualized using ECL Advance (GE Healthcare) and exposed to Hyperfilm MP (GE Healthcare). To ensure equal protein loading, each membrane was stripped and reprobed with anti-β-actin antibody.

Antitumor Activity in Vivo. Four-week-old female BALB/c-nu nude mice (15−18 g) were obtained from Shanghai SLAC Laboratory Animal Co., Ltd. (Shanghai, China). The animals were maintained under specific pathogen-free conditions with food and water supplied ad libitum at Zhejiang University, Traditional Chinese Medicine Laboratory Animal Center. Human colon adenocarcinoma HT-29 cells in logarithmic growth phase were resuspended in RPMI 1640 without fetal bovine serum at 1×10^7cells/mL and inoculated (0.2 mL) in the hypodermis of the pars dorsalis of each mouse. Once the HT-29 xenografts reached a size of ~300 mm^3, 18 mice were randomly assigned to either the control group or one of two treatment groups. Compounds **4l** and **1** were prepared in DMSO and injected intraperitoneally at 0.01 mL/g body weight to give a dose of 100 mg/kg. The drugs or vehicle was administered 3 times a week for 1 week. After completing the treatment schedule and the evaluation period, tumor-bearing mice were euthanized. Tumor volume was calculated by the formula $V = (LW^2)/2$ where L is the length and W is the width of the tumor nodules measured by vernier caliper. The study was approved by the Institutional Animal Ethical Committee of the Second Affiliated Hospital, School of Medicine, Zhejiang University (PRC).

Statistical Analysis. Unless indicated otherwise, the results are presented as the mean ± SEM. The differences between different treatments were analyzed using the two-sided Student's t test. P values lower than 0.05 were considered significant.

AUTHOR INFORMATION

Corresponding Author

*For R.R.: phone, 39-(0)532-455303; fax, 39-(0)532-455953; e-mail, rmr@unife.it. For P.G.B.: phone, 39-(0)532-455293; fax, 39-(0)532-455953; e-mail, pgb@unife.it. For G.V.: phone, 39-(0)49-8211451; fax, 39-(0)49-8211462; e-mail, giampietro.viola1@unipd.it.

ABBREVIATIONS USED

EWG, electron-withdrawing group; ERG, electron-releasing group; P-gp, P-glycoprotein; TFP, tri-(2-furyl)phosphine; MPF, M phase promoting factor; PI, propidium iodide; PS, phosphatidylserine; $\Delta\psi_{mt}$, mitochondrial transmembrane potential; JC-1, 5,5′,6,6′-tetrachloro-1,1′,3,3′-tetraethylbenzimidazolcarbocyanine; ROS, reactive oxygen species; HE, hydroethidine; H_2-DCFDA, 2,7 dichlorodihydrofluorescein diacetate; DCF, dichlorofluorescein; PARP, poly ADP-ribose polymerase; XIAP, X-linked inhibitor of apoptosis protein; ESI, electrospray ionization; PBS, phosphate buffered saline; SDS−PAGE, sodium dodecyl sulfate−polyacrylamide gel electrophoresis

REFERENCES

(1) (a) Downing, K. H. Structural basis for the interaction of tubulin with proteins and drugs that affect microtubule dynamics. *Annu. Rev. Cell Dev. Biol.* **2000**, *16*, 89−111. (b) Amos, L. A. Microtubule structure and its stabilisation. *Org. Biomol. Chem.* **2004**, *2*, 2153−2160. (c) Honore, S.; Pasquier, E.; Braguer, D. Understanding microtubule dynamics for improved cancer therapy. *Cell. Mol. Life Sci.* **2005**, *62*, 3039−3056.

(2) (a) Risinger, A. L.; Giles, F. J.; Mooberry, S. L. Microtubule dynamics as a target in oncology. *Cancer Treat. Rev.* **2008**, *35*, 255−261. (b) Kingston, D. G. Tubulin-interactive natural products as anticancer agents (1). *J. Nat. Prod.* **2009**, *72*, 507−515. (c) Dumantet, C.; Jordan, M. A. Microtubule-binding agents: a dynamic field of cancer therapeutics. *Nat. Rev. Drug Discovery* **2010**, *9*, 790−803. (d) Kanthou, C.; Tozer, G. M. Microtubule depolymerizing vascular disrupting agents: novel therapeutic agents for oncology and other pathologies. *Int. J. Exp. Pathol.* **2009**, *90*, 284−294.

(3) Pettit, G. R.; Singh, S. B.; Hamel, E.; Lin, C. M.; Alberts, D. S.; Garcia-Kendall, D. Isolation and structure of the strong cell growth and tubulin inhibitor combretastatin A-4. *Experentia* **1989**, *45*, 209−211.

(4) Lin, C. M.; Ho, H. H.; Pettit, G. R.; Hamel, E. Antimitotic natural products combretastatin A-4 and combretastatin A-2: studies on the mechanism of their inhibition of the binding of colchicine to tubulin. *Biochemistry* **1989**, *28*, 6984−6991.

(5) McGown, A. T.; Fox, B. W. Differential cytotoxicity of combretastatins A1 and A4 in two daunorubucin-resistant P388 cell lines. *Cancer Chemother. Pharmacol.* **1990**, *26*, 79−81.

(6) (a) Petit, I.; Karajannis, M. A.; Vincent, L.; Young, L.; Butler, J.; Hopper, A. T.; Shido, K.; Steller, H.; Chaplin, D. J.; Feldman, E.; Rafi, S. The microtubule-targeting agent CA4P regresses leukemic xenografts by disrupting interaction with vascular cells and mitochondrial-dependent cell death. *Blood* **2008**, *111*, 1951−1961. (b) Siemann, D. W.; Chaplin, D. J.; Walike, P. A. A review and update of the current status of the vasculature-disabling agent combretastatin-A4 phosphate (CA4P). *Expert Opin. Invest. Drugs* **2009**, *18*, 189−197. (c) Patterson, D. M.; Rustin, G. J. S. Combretastatin A-4 phosphate. *Drugs Future* **2007**, *32*, 1025−1032.

(7) (a) Tron, G. C.; Pirali, T.; Sorba, G.; Pagliai, F.; Busacca, S.; Genazzani, A. A. Medicinal chemistry of combretastatin A4: present and future directions. *J. Med. Chem.* **2006**, *49*, 3033−3044. (b) Chaudari, A.; Pandeya, S. N.; Kumar, P.; Sharma, P. P.; Gupta, S.; Soni, N.; Verma, K. K.; Bhardwaj, G. Combretastain A-4 analogues as anticancer agents. *Mini-Rev. Med. Chem.* **2007**, *12*, 1186−1205. (c) Hsieh, H. P.; Liou, J. P.; Mahindroo, N. Pharmaceutical design of antimitotic agents based on combretastatins. *Curr. Pharm. Des.* **2005**, *11*, 1655−1677. (d) Mahindroo, N; Liou, J. P.; Chang, J. Y.; Hsieh, H. P. Antitubulin agents for the treatment of cancer. A medicinal chemistry update. *Expert Opin. Ther. Pat.* **2006**, *16*, 647−691.

(8) Theeramunkong, S.; Caldarelli, A.; Massarotti, A.; Aprile, S.; Caprifoglio, D.; Zaninetti, R.; Teruggi, A.; Pirali, T.; Grosa, G.; Tron,

G. C.; Genazzani, A. A. Regioselective Suzuki coupling of dihaloheteroaromatic compounds as a rapid strategy to synthesize potent rigid combretastatin analogues. *J. Med. Chem.* **2011**, *54*, 4977−4986.

(9) (a) Ohsumi, K.; Hatanaka, T.; Fujita, K.; Nakagawa, R.; Fukuda, Y.; Nihai, Y.; Suga, Y.; Morinaga, Y.; Akiyama, Y.; Tsuji, T. Synthesis and antitumor activity of cis-restricted combretastatins 5-membered heterocyclic analogues. *Bioorg. Med. Chem. Lett.* **1988**, *8*, 3153−3158. (b) Wang, L.; Woods, K. W.; Li, Q.; Barr, K. J.; McCroskey, R. W.; Hannick, S. M.; Gherke, L.; Credo, R. B.; Hui, Y.-H.; Marsh, K.; Warner, R.; Lee, J. Y.; Zielinski-Mozng, N.; Frost, D.; Rosenberg, S. H.; Sham, H. L. Potent, orally active heterocycle-based combretastatin A-4 analogues: synthesis, structure−activity relationship, pharmaokinetics, and in vivo antitumor activity evaluation. *J. Med. Chem.* **2002**, *45*, 1697−1711.

(10) (a) Bonezzi, K.; Taraboletti, G.; Borsotti, P.; Bellina, F.; Rossi, R.; Gavazzi, R. Vascular disrupting activity of tubulin-binding 1,5-diaryl-1*H*-imidazoles. *J. Med. Chem.* **2009**, *52*, 7906−7910. (b) Schobert, R.; Biersack, B.; Dietrich, A.; Effenberger, K.; Knauer, S.; Mueller, T. 4-(3-Halo/amino-4,5-dimethoxyphenyl)-5-aryloxazoles and *N*-methylimidazoles that are cytotoxic against combretastatin A-4 resistant tumor cels and vascular disrupting in a cis-platin resistant germ cell tumor model. *J. Med. Chem.* **2010**, *53*, 6595−6002.

(11) (a) Kaffy, J.; Pontikis, R.; Carrez, D.; Croisy, A.; Monneret, C.; Florent, J.-C. Isoxazole-type derivatives related to combretastatin A-4, synthesis and biological evaluation. *Bioorg. Med. Chem.* **2006**, *14*, 4067−4077. (b) Lee, S.; Kim, J. N.; Lee, H. K.; Yoon, K. S.; Shin, K. D.; Kwon, B.-M.; Han, D. C. Biological evaluation of KRIBB3 analogs as a microtubule polymerization inhibitor. *Bioorg. Med. Chem. Lett.* **2011**, *21*, 977−979.

(12) Wu, M.; Li, W.; Yang, C.; Chen, D.; Ding, J.; Chen, Y.; Lin, L.; Xie, Y. Synthesis and activity of combretastatin A-4 analogues: 1,2,3-thiadiazoles as potent antitumor agents. *Bioorg. Med. Chem. Lett.* **2007**, *17*, 869−873.

(13) (a) Odlo, K.; Hntzen, J.; Fournier dit Chabert, J.; Ducki, S.; Gani, O. A. B. S. M.; Sylte, I.; Skrede, M.; Florenes, V. A.; Hansen, T. V. 1,5-Disubstituted 1,2,3-triazoles as cis-restricted analogues of combretastatin A-4: synthesis, molecular modeling and evaluation as cytotoxic agents and inhibitors of tubulin. *Bioorg. Med. Chem.* **2008**, *16*, 4829−4838. (b) Zhang, Q.; Peng, Y.; Wang, X. I.; Keeman, S. M.; Aurora., S.; Welsh, W. J. Highly potent triazole-based tubulin polymerization inhibitors. *J. Med. Chem.* **2007**, *50*, 749−754. (c) Romagnoli, R.; Baraldi, P. G.; Cruz-Lopez, O.; Lopez-Cara, C.; Carrion, M. D.; Brancale, A.; Hamel, E.; Chen, L.; Bortolozzi, R.; Basso, G.; Viola, G. Synthesis and antitumor activity of 1,5-disubstituted 1,2,4-triazoles as cis-restricted combretastatin analogs. *J. Med. Chem.* **2010**, *53*, 4248−4258.

(14) Only one analogue with a tetrazole ring, corresponding to 1-(3,4,5-trimethoxyphenyl)-5-(4-methoxy,3-aminophenyl)-1*H*-tetrazole, has been reported by Otsumi et al. (ref 9a). This compound showed potent antitubulin activity (IC_{50} = 2 μM) as well as cytotoxicty (IC_{50} = 7.2 nM) against the colon 26 murine tumor cell line.

(15) (a) Cushman, M.; Nagarathnam, D.; Gopal, D.; He, H.-M.; Lin, C. M.; Hamel, E. Synthesis and evaluation of analogues of (*Z*)-1-(4-methoxyphenyl)-2-(3,4,5-trimethoxyphenyl)ethene as potential cytotoxic and antimitotic agents. *J. Med. Chem.* **1992**, *35*, 2293−2306. (b) Gaukroger, K.; Hadfield, J. A.; Lawrence, N. J.; Nlan, S.; McGown, A. T. Structural requirements for the interaction of combretastatins with tubulin: How important is the trimethoxy unit? *Org. Biomol. Chem.* **2003**, *1*, 3033−3037.

(16) For compound **7a** see the following: Potewar, T. M.; Siddiqui, S. A.; Lahoti, R. J.; Srinivasan, K. V. Efficient and rapid synthesis of 1-substituted-1*H*-1,2,3,4-tetrazoles in the acidic ionic liquid 1-*n*-butylimidazolium tetrafluoroborate. *Tetrahedron Lett.* **2007**, *48*, 1721−1724. For compound **7b** see the following: Vorobiov, A. N.; Gaponik, P. N.; Petrov, P. T.; Ivashkevich, O. A. One-pot syntheses of 5-amino-1-aryltetrazole derivatives. *Synthesis* **2010**, 1307−1312.

(17) Satoh, Y.; Marcopulos, N. Application of 5-lithiotetrazoles in organic synthesis. *Tetrahedron Lett.* **1995**, *36*, 1679−1682.

(18) Yi, K. Y.; Yoo, S. Synthesis of 5-aryl and vinyl tetrazoles by the palladium-catalyzed cross-coupling reaction. *Tetrahedron Lett.* **1995**, *36*, 1679−1682.

(19) Spulak, M.; Lubojacky, R.; Senel, P.; Kunes, J.; Pour, M. Direct C-H arylation and alkenylation of 1-substituted tetrazoles: phosphine as stabilizing factor. *J. Org. Chem.* **2010**, *75*, 241−244.

(20) (a) Hamel, E. Evaluation of antimitotic agents by quantitative comparisons of their effects on the polymerization of purified tubulin. *Cell Biochem. Biophys.* **2003**, *38*, 1−21. (b) Verdier-Pinard, P.; Lai, J.-Y.; Yoo, H.-D.; Yu, J.; Marquez, B.; Nagle, D. G.; Nambu, M.; White, J. D.; Falck, J. R.; Gerwick, W. H.; Day, B. W.; Hamel, E. Structure−activity analysis of the interaction of curacin A, the potent colchicine site antimitotic agent, with tubulin and effects of analogs on the growth of MCF-7 breast cancer cells. *Mol. Pharmacol.* **1998**, *53*, 62−67.

(21) Szakács, G.; Paterson, J. K.; Ludwig, J. A.; Booth-Genthe, C.; Gottesman, M. M. Targeting multidrug resistance in cancer. *Nat. Rev. Drug Discovery* **2006**, *5*, 219−234.

(22) Baguley, B. C. Multidrug resistance mechanism in cancer. *Mol. Biotechnol.* **2010**, *46*, 308−316.

(23) Dupuis, M.; Flego, M.; Molinari, A.; Cianfriglia, M. Saquinavir induces stable and functional expression of the multidrug transporter P-glycoprotein in human CD4 T-lymphoblastoid CEM rev cells. *HIV Med.* **2003**, *4*, 338−345.

(24) Toffoli, G.; Viel, A.; Tuimoto, I.; Bisconti, G.; Rossi, G.; Baoiocchi, M. Pleiotropic-resistant phenotype is a multifactorial phenomenon in human colon carcinoma cell lines. *Br. J. Cancer* **1991**, *63*, 51−56.

(25) Martello, L. A.; Verdier-Pinard, P.; Shen, H. J.; He, L.; Torres, K.; Orr, G. A.; Horwitz, S. B. Elevated level of microtubule destabilizing factors in a Taxol-resistant/dependent A549 cell line with an alpha-tubulin mutation. *Cancer Res.* **2003**, *63*, 448−454.

(26) Clarke, P. R.; Allan, L. A. Cell-cycle control in the face of damage: a matter of life or death. *Trends Cell Biol.* **2009**, *19*, 89−98.

(27) Donzelli, M.; Draetta, G. F. Regulating mammalian checkpoints through Cdc25 inactivation. *EMBO Rep.* **2003**, *4*, 671−677.

(28) Kiyokawa, H.; Ray, D. In vivo roles of Cdc25 phosphatases: biological insight into the anti-cancer therapeutic targets. *Anti-Cancer Agents Med. Chem.* **2008**, *8*, 832−836.

(29) Vermes, I.; Haanen, C.; Steffens-Nakken, H.; Reutelingsperger, C. A novel assay for apoptosis. Flow cytometric detection of phosphatidylserine expression on early apoptotic cells using fluorescein labelled annexin V. *J. Immunol. Methods* **1995**, *184*, 39−51.

(30) (a) Ly, J. D.; Grubb, D. R.; Lawen, A. The mitochondrial membrane potential ($\Delta\psi_m$) in apoptosis: an update. *Apoptosis* **2003**, *3*, 115−128. (b) Green, D. R.; Kroemer, G. The pathophysiology of mitochondrial cell death. *Science* **2005**, *305*, 626−629.

(31) Cai, J.; Jones, D. P. Superoxide in apoptosis. Mitochondrial generation triggered by cytochrome *c* loss. *J. Biol. Chem.* **1998**, *273*, 11401−11404.

(32) (a) Rothe, G.; Valet, G. Flow cytometric analysis of respiratory burst activity in phagocytes with hydroethidine and 2′,7′-dichlorofluorescein. *J. Leukocyte Biol.* **1990**, *47*, 440−448. (b) Nohl, H.; Gille, L.; Staniek, K. Intracellular generation of reactive oxygen species by mitochondria. *Biochem. Pharmacol.* **2005**, *69*, 719−723.

(33) Denault, J.-B.; Salvesen, G. S. Caspases: keys in the ignition of cell death. *Chem. Rev.* **2002**, *102*, 4489−4499.

(34) Porter, A. G.; Janicke, R. U. Emerging role of caspase-3 in apoptosis. *Cell Death Differ.* **1999**, *6*, 99−104.

(35) Mollinedo, F.; Gajate, C. Microtubules, microtubule-interfering agents and apoptosis. *Apoptosis* **2003**, *8*, 413−450.

(36) Dingemans, T.; Photinos, D. J.; Samulski, E. T.; Terzis, A. F.; Wutz, C. Ordering of apolar and polar solutes in nematic solvents. *J. Chem. Phys.* **2003**, *118*, 7046−7061.

(37) Viola, G.; Fortunato, E.; Cecconet, L.; Del Giudice, L.; Dall'Acqua, F.; Basso, G. Central role of mitochondria and p53 in PUVA-induced apoptosis in human keratinocytes cell line NCTC-2544. *Toxicol. Appl. Pharmacol.* **2008**, *227*, 84−96.

(38) Ravelli, R. B. G.; Gigant, B.; Curmi, P. A.; Jourdain, I.; Lachkar, S.; Sobel, A.; Knossow, M. Insight into tubulin regulation from a complex with colchicine and a stathmin-like domain. *Nature* **2004**, *428*, 198−202.
(39) *Molecular Operating Environment (MOE 2008.10)*; Chemical Computing Group, Inc.: Montreal, Quebec, Canada; http://www.chemcomp.com.
(40) Korb, O.; Stützle, T.; Exner, T. E. PLANTS: Application of Ant Colony Optimization to Structure-Based Drug Design. In *Ant Colony Optimization and Swarm Intelligence*, 5th International Workshop, ANTS 2006, Brussels, Belgium, Sep 4−7, 2006; Dorigo, M., Gambardella, L. M., Birattari, M., Martinoli, A., Poli, R., Sttzle, T., Eds.; Springer: Berlin, Germany, 2006; LNCS 4150, pp 247−258.